Hydrological variability in southeastern Patagonia and explosive volcanic activity in the southern Andean Cordillera during Oxygen Isotope Stage 3 and the Holocene inferred from lake sediments of Laguna Potrok Aike, Argentina

Haberzettl, Torsten; Kück, Barbara; Wulf, Sabine; Anselmetti, Flavio S.; Ariztegui, Daniel; Corbella, Hugo; Fey, Michael; Janssen, Stephanie; Lücke, Andreas; Mayr, Christoph; Ohlendorf, Christian; Schäbitz, Frank; Schleser, Gerhard H.; Wille, Michael [**and 1 more**]

Available online at www.sciencedirect.com
ScienceDirect
Palaeogeography, Palaeoclimatology, Palaeoecology 259 (2008) 213–229
PALAEO
www.elsevier.com/locate/palaeo

Hydrological variability in southeastern Patagonia and explosive volcanic activity in the southern Andean Cordillera during Oxygen Isotope Stage 3 and the Holocene inferred from lake sediments of Laguna Potrok Aike, Argentina

Torsten Haberzettl [a,b,*], Barbara Kück [a], Sabine Wulf [c,d], Flavio Anselmetti [e], Daniel Ariztegui [f], Hugo Corbella [g], Michael Fey [a], Stephanie Janssen [h], Andreas Lücke [i], Christoph Mayr [i,j], Christian Ohlendorf [a], Frank Schäbitz [h], Gerhard H. Schleser [i], Michael Wille [h], Bernd Zolitschka [a]

[a] *Geomorphology and Polar Research (GEOPOLAR), Institute of Geography, University of Bremen, Celsiusstr. FVG-M, D-28359 Bremen, Germany*
[b] *Sedimentology and Environmental Geology, Geoscience Center, University of Göttingen, Goldschmidtstr. 3, D-37077 Göttingen, Germany*
[c] *GeoForschungsZentrum Potsdam, Section 3.3 - Climate dynamics and sediments, Telegrafenberg, D-14473 Potsdam, Germany*
[d] *Institute for Geophysics, Jackson School of Geosciences, The University of Texas at Austin, J.J. Pickle Research Campus, Bldg. 196, 10100 Burnet Rd., Austin, Texas 78758-4445, USA*
[e] *Geological Institute, ETHZ, Universitätsstr. 16, CH-8092 Zürich, Switzerland*
[f] *Institute Forel and Department of Geology and Paleontology, Rue des Maraîchers 13, CH-1205 Geneva, Switzerland*
[g] *Argentine Museum of Natural History, Avenida Angel Gallardo 470, Buenos Aires, Argentina*
[h] *Seminar for Geography and Education, University of Cologne, Gronewaldstr. 2, D-50931 Cologne, Germany*
[i] *Institute of Chemistry and Dynamics of the Geosphere V: Sedimentary Systems, Research Center Jülich, D-52425 Jülich, Germany*
[j] *GeoBio-Center^{LMU}, Ludwig-Maximilians-Universität, Richard-Wagner-Str. 10, D-80333 Munich, Germany*

Received 28 October 2005; accepted 14 August 2007

Abstract

Seismic reflection studies in the maar lake Laguna Potrok Aike (51°58′ S, 70°23′ W) revealed an erosional unconformity associated with a sub-aquatic lake-level terrace at a water depth of 30m. Radiocarbon-dated, multi-proxy sediment studies of a piston core from this location indicate that the sediment below this discontinuity has an age of 45kyr BP (Oxygen Isotope Stage 3), and was deposited during an interval of high lake level. In comparison to the Holocene section, geochemical indicators of this older part of the record either point towards a different sediment source or to a different transport mechanism for Oxygen Isotope Stage 3 sediments. Holocene sedimentation started again before 6790cal. yr BP, providing a sediment record of hydrological variability until the present. Geochemical and isotopic data indicate a fluctuating lake level until 5310cal. yr BP. During the late Holocene the lake level shows a receding tendency. Nevertheless, the lake level did not drop below the 30m terrace to create another

* Corresponding author. Sedimentology and Environmental Geology, Geoscience Center, University of Göttingen, Goldschmidtstr. 3, D-37077 Göttingen, Germany. Fax: +49 551 397996.
E-mail address: Torsten.Haberzettl@geo.uni-goettingen.de (T. Haberzettl).

0031-0182/$ - see front matter
doi:10.1016/j.palaeo.2007.10.008

unconformity. The geochemical characterization of volcanic ashes reveals evidence for previously unknown explosive activity of the Reclús and Mt. Burney volcanoes during Oxygen Isotope Stage 3.

Keywords: Geochemistry; Lacustrine sediments; Lake level changes; Tephrostratigraphy; Argentina; Palaeoclimate

1. Introduction

Major gaps of palaeoclimatic information exist during Oxygen Isotope Stage 3 (OIS 3) in the marine sector around South America as well as in high-resolution terrestrial records over large parts of this continent (Voelker, 2002). Such information is critically needed in order to compare southern-hemisphere climate with the better known climate history from the tropics and the northern hemisphere. This permits an assessment of possible synchronicity of global climate events in the past, and a validation of global climate models. Climatic information from terrestrial archives in South America covering OIS 3, however, is limited to latitudes north of 43° S (Voelker, 2002). The southernmost sites comprise pollen records from several sites, including a mire at Taiquemó (42°10′ S, 73°36′ W) on Isla Grande de Chiloé in Chile (Heusser et al., 1999; Heusser and Heusser, 2006), and a fen at Fundo Nueva Braunau (40°17′ S, 73°05′ W, Heusser et al., 2000), as well as tree-ring studies based on sub-fossil tree remnants found at Seno Reloncaví (40°00′ to 42°30′ S, 71°30′ to 74°00′ W), both in the southern Lake District of Chile (Roig et al., 2001). Farther south, climatological information covering this time interval originates from Antarctic ice cores (Petit et al., 1990; 1999). Hence, a high-resolution sediment record from Laguna Potrok Aike (51°58′ S, 70°23′ W) (Figs. 1 and 2) covering OIS 3 would be a critical step towards bridging the gap between these continental records. One aim of this paper therefore is to investigate the hydrological variability in southeastern Patagonia on the basis of lacustrine sediments from Laguna Potrok Aike during the Holocene and OIS 3.

Additionally, the identification of ash layers will allow the refinement of the regional tephrostratigraphy. During the Late Quaternary southern Patagonia was influenced by intensive volcanism that occurred along the Southern Andes in two separate volcanic zones, i.e., the Southern Volcanic Zone (SVZ) and the Austral Volcanic Zone (AVZ) (Stern et al., 1984). To the north, the Hudson volcano in the southern part of the Southern Volcanic Zone (SSVZ, 46° S) erupted basaltic and trachyandesitic to rhyodacitic pyroclastic material. In the south, the stratovolcanoes of the AVZ (49°–54° S) produced many tephra eruptions of andesitic–dacitic to rhyolitic composition (Stern and Kilian, 1996). Most of those eruptions were confined to the Lautaro, Viedma and Aguilera volcanoes in the northern part (NAVZ) as well as to Mt. Burney and Reclús in the southern part of the AVZ (Auer, 1974; Stern, 1990). The Holocene explosive history of SSVZ and AVZ volcanoes has been characterized on the basis of chemical discrimination of numerous distal tephra layers detected in terrestrial sediment records from Chile and Argentina (Auer, 1974; Stern, 1990; Stern and Kilian, 1996; Haberle and Lumley, 1998; Markgraf et al., 2003). Tephra ages were estimated indirectly using numerous radiocarbon dates that are bracketing the respective tephras. Although widespread in Patagonia, volcanic ashes older than Holocene have not been the focus of detailed studies. Up to now, geochemical characterization of tephras erupted during OIS 3 have only been performed further north (Toms et al., 2004). Those investigations identified volcanic ashes from the Quizapu volcano at the northern limit of the SVZ (Toms et al., 2004) confirming the existence of volcanic activity in the SVZ during that time.

2. Site description

The maar lake Laguna Potrok Aike is located in southeastern Patagonia (Fig. 1). This environment is characterized by a strong precipitation gradient from west to east with ca. 170mm/yr of precipitation at the lake. Climate in this area is dominated by the westerly wind constituting more than 50% of all wind directions and reaching mean monthly wind speeds of 9m/s during early summer (Endlicher, 1993).

The circular lake has a maximum diameter of 3470m. The catchment area (> 200km^2) reaches far south. Nevertheless, stream run-off only occurs episodically through a few gullies and canyons. In summer 2002, the lake level was at 113m a.s.l. and the maximum water depth was approximately 100m (Haberzettl et al., 2005). The lake is surrounded by well-preserved sub-aerial as well as sub-aquatic lake-level terraces formed by wave action. Lacking permanent surface inflow and outflow, Laguna Potrok Aike responds rapidly to changes in the precipitation/evaporation ratio, with rising lake levels in times of wetter climatic conditions and falling lake levels during drier periods (Haberzettl et al., 2005). Further details about Laguna Potrok Aike are provided elsewhere

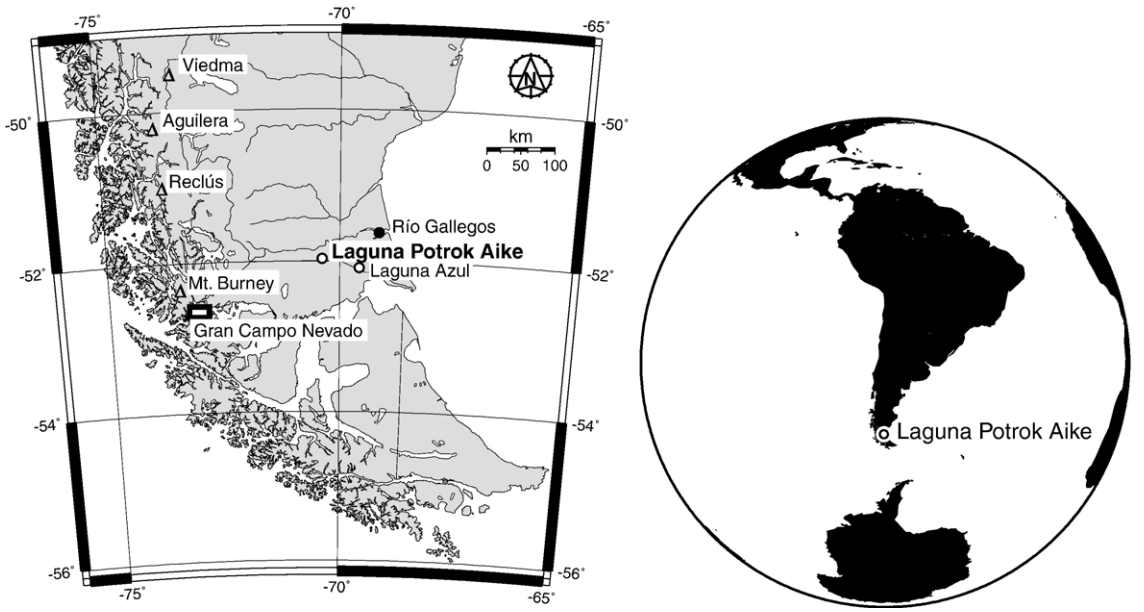

Fig. 1. Location of the research area in southern South America and other sites mentioned in the text. Maps were created with OMC (Weinelt, 1996–2004).

(Schäbitz et al., 2003; Zolitschka et al., 2004; 2006; Haberzettl et al., 2005, 2006, 2007; Haberzettl, 2006).

3. Field and laboratory methodology

3.1. Field methods

A seismic survey of the lake consisting of 70km of high-resolution single-channel seismic data was acquired in February 2003 with a 3.5kHz pinger system characterized by a vertical resolution of 10cm. The survey was performed with a steel-hulled catamaran with a conventional GPS-based navigation. Seismic data were stored digitally in SEG-Y format allowing further processing and interpretation. A 2–6.5kHz band-pass filter was applied to the data.

Two overlapping sediment cores of 5m length (PTA03/6-1 to PTA03/6-5 and PTA03/6-6 to PTA03/6-10 constituting the core PTA03/6, Fig. 2) were retrieved using a hand-driven UWITEC piston coring system (www.uwitec.at, acrylic glass tubes, I.D. 60mm) from a lake-level terrace approximately 30m below the present lake surface. This was detected during the seismic survey (Fig. 2). Cores were cut into one-meter sections on board of the research vessel. Field length of the entire core PTA03/6 comprising all sections was 981cm.

3.2. Non-destructive laboratory methods

In the laboratory, sediment cores were stored in darkness at 4°C, before being split, photographed and described lithologically. Additionally, smear slides were prepared at eight-centimeter intervals and at depths with lithological differences for microscopic inspection.

A non-destructive core-scanning method was applied to all sections using a CORTEX (Corescanner Texel) XRF-scanner, which provides qualitative analyses of the chemical elements K, Ca, Ti, V, Cr, Mn, Fe, Co, Ni, Cu, Zn, Sr and Pb (Jansen et al., 1998). The Ca-profile obtained by XRF scanning, and photographs including macroscopic marker layers were used for correlation of the overlapping core sections and for establishment of a composite sediment profile. After correlation the total sub-bottom depth of the core was 900cm.

A second non-destructive method applied on the split cores was magnetic-susceptibility scanning, measured with a point sensor in 1-cm resolution using a Bartington sensor (type MS2E).

3.3. Destructive laboratory methods

Cores were sub-sampled continuously and volumetrically in 1-cm intervals. All volumetric sediment samples were freeze-dried for determination of dry density and water content. Dried samples were ground in a mortar and homogenized prior to measuring total nitrogen (TN), total carbon (TC) and total sulfur (TS) in 4-cm increments using a CNS elemental analyzer (EuroEA, Eurovector). Sub-samples were subsequently treated with 3% and 20% HCl at 80°C to remove any carbonates and then measured with the CNS analyzer again for

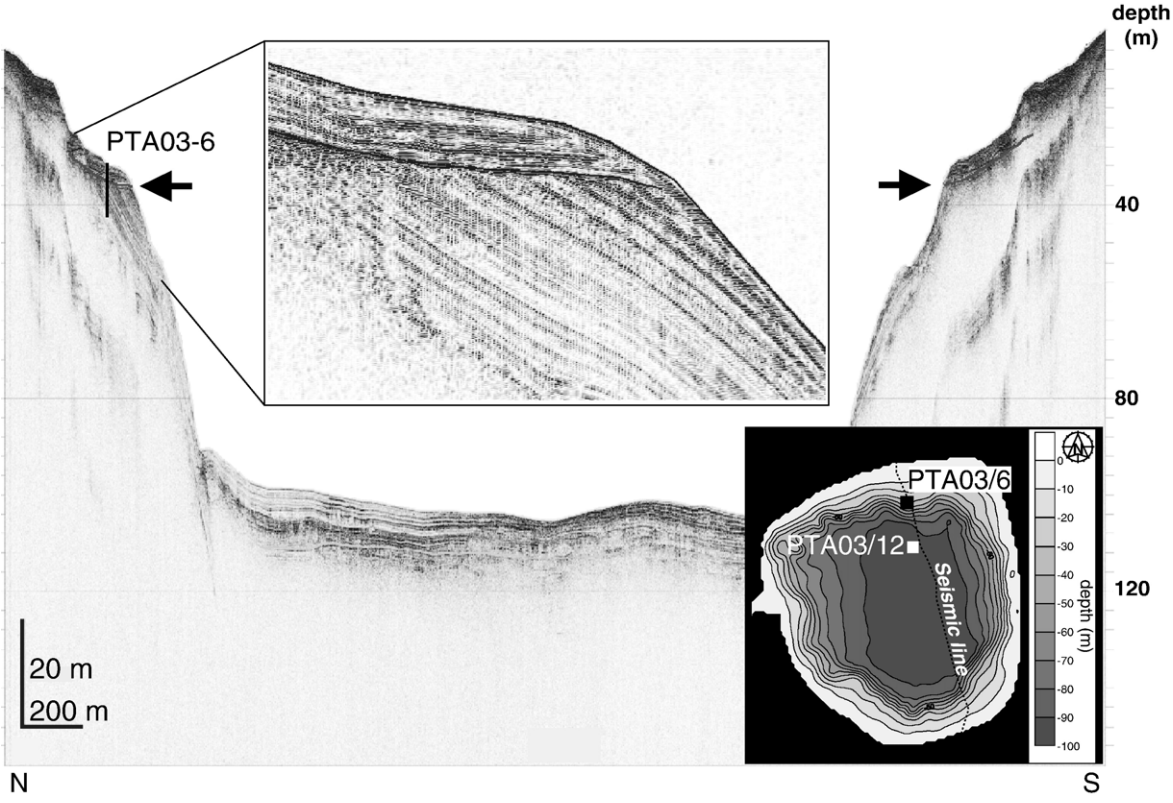

Fig. 2. Seismic profile of Laguna Potrok Aike performed with a 3.5 kHz system (note vertical exaggeration). The unconformity visible in the seismic profile is displayed in the blow-up in the center and highlighted with arrows in the profile. The location of core PTA03/6 is indicated in the bathymetric map and in the profile. The location of the core from the center of Laguna Potrok Aike (PTA03/12), used for comparative reasons, is only indicated in the bathymetry.

determination of total organic carbon (TOC). Total inorganic carbon (TIC) was calculated as the difference between TC and TOC. A preliminary screening with eight-centimeter increments showed that TIC was absent in all samples below 311cm. Therefore, TOC was considered to be equal to TC for the samples from this section. At depths that show a larger variability in specific parameters, measurement resolution was increased to 1-cm intervals. Bulk mineralogy was determined for selected samples using X-ray diffraction (XRD) techniques (Philips X´Pert Pro MD equipped with an X'Celerator Detector-Array).

Grain-size analyses were performed using a laser diffraction particle size analyzer (LS 200, Coulter) equipped with a variable-speed fluid module which measures particles from 0.4 to 2000μm. Sub-samples taken every 5cm were pooled for each 1-m section. In a section containing, according to the measured parameters, an unconformity, pooled samples were taken from above and immediately below the unconformity as well as from the lowest part of the section. Prior to analyses, samples were treated with H_2O_2 to remove the organic fraction, HCl to remove carbonates and NaOH to remove biogenic silica. Chemical dispersion was performed using Calgon ($(NaPO_3)n$).

For analyses of carbon isotope ratios of organic matter ($\delta^{13}C_{org}$) in 8-cm intervals, samples were treated with 5% HCl for 6h in a water bath at 50°C to remove carbonates, afterwards rinsed with deionized water until pH was neutral and freeze-dried. Samples were combusted at 1080°C in an elemental analyzer (EuroEA, Eurovector) and resulting CO_2 gas was analyzed with an IRMS (Isoprime, Micromass). Isotope ratios are reported as conventional δ-values (in ‰) with $\delta = (R_s/R_{st}\ 1) * 1000$, where R_s and R_{st} are the $^{13}C/^{12}C$ ratios of the sample and an international standard (Vienna-Pee Dee Belemnite, VPDB), respectively.

3.4. Chronology

Plant macro-remains were picked out for AMS ^{14}C dating and gastropods for later taxonomic determination. In total, five samples were selected for AMS ^{14}C age determination carried out at the Poznan Radiocarbon

Laboratory (Poland). Radiocarbon analyses were performed on sieved samples containing remains of aquatic macrophytes (> 100μm). Radiocarbon ages were calibrated using the southern-hemisphere calibration curve (McCormac et al., 2004) labeled as "shcal.", as well as with the northern-hemisphere calibration curve (Reimer et al., 2004) marked as "nhcal.", to facilitate comparisons with other archives, using the software CALIB 5.0.2 (Stuiver and Reimer, 1993; Stuiver et al., 2005).

3.5. Tephrochronology

Tephras have been characterized geochemically and microscopically in order to define the volcanic sources. For comparison, tephra samples from the Hudson, Reclús and Aguilera/Lautaro volcanoes (Gilli et al., 2001; 2005; Gilli, 2003; Markgraf et al., 2003) obtained from the sediment records of Lago Cardiel (48°57′ S, 71°26′ W) were analyzed as well. Tephra samples were carefully cleaned with 30% H_2O_2 to remove organic matter and surface coatings, and dried with ethanol. Major-element chemistry of single glass shards was determined on the basis of polished thin sections by electron-probe micro-analyses (EPMA) using a CAMECA SX100 instrument at GFZ Potsdam. The operating conditions for measurements were 15kV accelerating voltage, 20nA beam current, a defocused beam of 15μm diameter and peak counting times of 20s except for Na (10s). Instrumental calibration used interlaboratory natural mineral and glass (Lipari obsidian) reference materials (Hunt and Hill, 1996). At least ten glass shards per tephra were measured according to

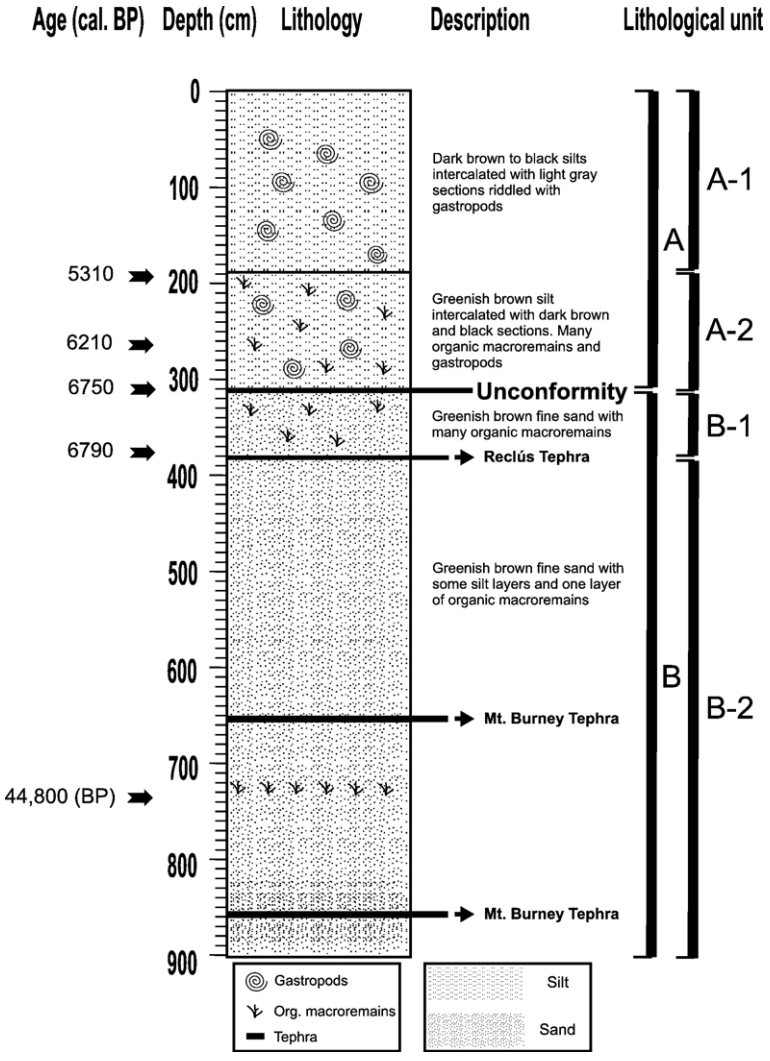

Fig. 3. Lithology of core PTA03/6 from Laguna Potrok Aike including ages derived from the age model.

Table 1
AMS radiocarbon dating carried out on stems of aquatic mosses

Lab. no.	Sediment depth	^{14}C age (BP)	Error	shcal. median age (BP)	Error to present (2σ)	Error to past (2σ)	nhcal. median age (BP)	Error to present (2σ)	Error to past (2σ)	Age derived from age model used for interpretation (cal. BP)	Sediment depth
Poz-6096	191 cm	4680	±40	5390	315	185	5400	85	175	5310	191 cm
Poz-6166	266 cm	5320	±50	6050	130	130	6100	150	170	6210	266 cm
Poz-6167	311 cm	6040	±40	6820	125	140	6890	120	105	6750	311 cm
Poz-6097 (only 0.23 mg C)	372 cm	5910	±50	6670	120	165	6730	95	150	6790	372 cm
Poz-6098	728 cm	44,800	±2000							44,800 (years BP)	728 cm

Radiocarbon ages were calibrated with the southern-hemisphere calibration curve (shcal., McCormac et al., 2004) as well as with the northern-hemisphere calibration curve (nhcal., Reimer et al., 2004) for comparative reasons using the software CALIB 5.0.2 (Stuiver and Reimer, 1993, Stuiver et al., 2005). The ages derived from the age model are given in cal. BP and are used for interpretation.

the homogeneity of samples. Individual analyses of glass shards with total oxide sums lower than 95wt.% have been excluded. The data of accepted analyses of individual tephra layers were recalculated to 100wt.% and given as a mean with 1σ standard deviation of *n* glass shards. Petrological classification is based on the Total Alkali–Silica diagram (Le Bas et al., 1986).

4. Results

4.1. Seismic reflection data

High-resolution seismic studies revealed an unconformity in a sub-aquatic lake-level terrace of Laguna Potrok Aike. The terrace is located approximately 30m below the present lake surface and both the unconformity and the terrace can be traced around the lake. The unconformity is characterized by 3 to 4m of almost horizontally layered or gently lakeward dipping layered sediments above and sediments following the morphology of the ancient lake by steeply dipping towards the lake center below (Fig. 2).

4.2. Lithology

In the core PTA03/6 (Fig. 2) two major lithological units can be distinguished, which are separated by the unconformity at 311cm (Fig. 3). Unit A (above the

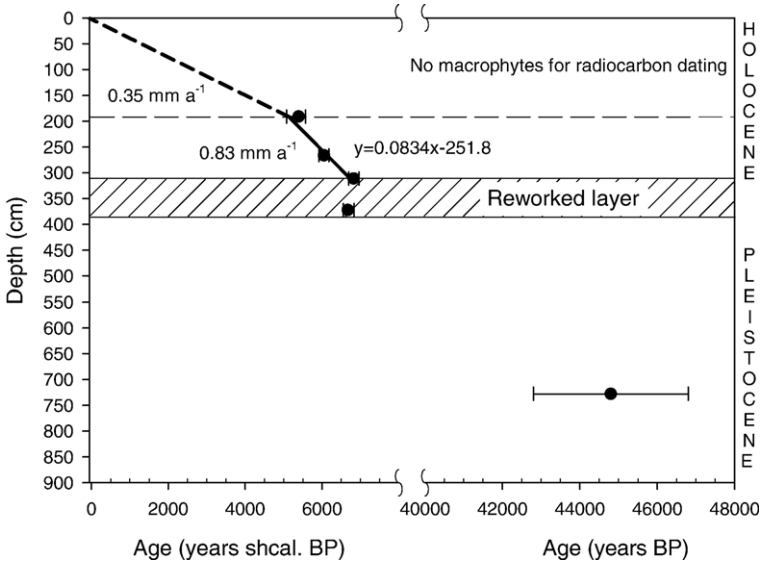

Fig. 4. Age model based on radiocarbon dates. Holocene dates are calibrated with CALIB 5.0.2 (Stuiver and Reimer, 1993; Stuiver et al., 2005). Each calibration was performed with the southern-hemisphere calibration curve and is displayed as median of the 2σ-probability distribution with error bars. The Pleistocene date is displayed as ^{14}C yr BP.

unconformity, 0–311cm) consists of dark-brown to black silts, whereas unit B (below the unconformity, 312–900cm) is composed of greenish-brown fine sands (Figs. 3 and 7). Both lithological units can be subdivided into two separate sub-units: A-1, A-2 and B-1, B-2 (Fig. 3). A-1 (0–190cm) consists of silt with abundant gastropods and A-2 (191–311cm) of silt with gastropods and, in addition, abundant plant debris. Unit B-1 (312–378cm) is characterized by the absence of gastropods but the presence of many organic macro-remains (moss shoots and plant debris), whereas in unit B-2 (379–900cm) macro-remains only occur in one layer at a depth of 728cm (Fig. 3). The boundary between sub-units B-1 and B-2 is marked by a white tephra layer at 379cm sediment depth. Further down-core, within B-2, two other volcanic ashes have been detected in sediment depths of 643cm and 859cm (Fig. 3).

4.3. Chronology

4.3.1. Radiocarbon dating

The AMS ^{14}C dating of sediment core PTA03/6 reveals ages between 4680 and 44,800yr BP (Table 1, Fig. 4). The oldest radiocarbon age therefore was not calibrated as it is beyond the calibration curves of CALIB 5.0.2 (McCormac et al., 2004; Reimer et al., 2004; Stuiver and Reimer, 1993; Stuiver et al., 2005). Hence, the oldest age is displayed uncalibrated in ^{14}C yr BP (Figs. 3 and 4, Table 1). The Holocene section was only dated in lithological unit A-2 and comprises the time interval between 4680±40yr BP ($5390^{+175}/_{-315}$ shcal. yr BP) and 6040±40yr BP ($6820^{+140}/_{-125}$ shcal. yr BP) as in unit A-1 no macro-remains for dating were available. The absence of a hard-water effect in the sediments of Laguna Potrok Aike has been demonstrated in an earlier study (Haberzettl et al., 2005).

4.3.2. Tephrochronology

Three previously unknown tephra layers have been identified in the lower part of PTA03/6 (Fig. 3). The youngest tephra at 379cm sediment depth is a 1.5-cm-thick, fine-grained (maximum grain size d_{max} 100μm) white ash layer that directly underlies lithological unit B-1. Glass shards forming the essential phase of tephra components reveal two different major-element chemistries: the main glass population is dacitic in composition, showing relatively high aluminum concentrations (> 15wt.%), while the secondary phase displays a rhyolitic composition with relatively high potassium values (Table 2). Minerals are rare and comprise plagioclase, orthopyroxene, amphibole and apatite phenocrysts. Sporadically, corroded xenocrysts of quartz, biotite and clinopyroxene are present displaying remaining components of granodioritic rock fragments.

Table 2
Mean major oxide concentrations of glass shards extracted from the tephra layers of core PTA03/6

Tephra	379 cm		643 cm	859 cm
	Glass type A	Glass type B		
SiO_2	70.19 (0.59)	74.52 (0.69)	72.69 (0.80)	74.26 (1.33)
TiO_2	0.56 (0.03)	0.12 (0.02)	0.34 (0.03)	0.23 (0.02)
Al_2O_3	15.23 (0.36)	12.43 (0.17)	13.39 (0.18)	12.99 (0.24)
FeO	2.79 (0.14)	0.99 (0.01)	1.94 (0.09)	1.39 (0.09)
MnO	0.05 (0.03)	0.03 (0.01)	0.05 (0.02)	0.04 (0.02)
MgO	0.84 (0.06)	0.14 (0.00)	0.49 (0.02)	0.37 (0.03)
CaO	3.08 (0.24)	1.17 (0.04)	2.26 (0.07)	1.79 (0.09)
Na_2O	3.59 (0.13)	3.01 (0.18)	3.54 (0.20)	3.79 (0.30)
K_2O	2.24 (0.07)	3.16 (0.12)	1.48 (0.02)	1.65 (0.11)
P_2O_5	0.11 (0.05)	0.04 (0.03)	0.06 (0.03)	0.05 (0.03)
Cl	0.13 (0.01)	0.17 (0.01)	0.19 (0.02)	0.17 (0.03)
Total	98.81	95.76	96.42	96.72
	$n=10$	$n=2$	$n=11$	$n=8$

n=number of shards analyzed. 1σ standard deviations are shown as numbers in parentheses.

Tephra layers at 643cm and 859cm sediment depth are both white ash deposits of 1cm thickness. The upper is mainly made up of fine-grained (d_{max} 100μm) vitric components which are characterized by a homogeneous low-K-rhyolitic chemistry (Table 2). Its mineral assemblage comprises plagioclase, orthopyroxene and rare amphibole phenocrysts. The lower tephra, in contrast, is a coarser-grained pumice deposit (d_{max} 300μm) that additionally contains rare biotite and Fe–Ti-oxide phenocrysts. Vitric components (microcrysts-bearing pumices and low vesicular glass shards) show a similar but slightly more silicic low-K-rhyolitic composition than the tephra at 643cm (Table 2).

4.4. Sediment analyses

4.4.1. Lithological unit B (below unconformity visible in lithology)

Below an unconformity visible in the lithology at 311cm, values for magnetic susceptibility and dry density are much higher (Fig. 5) than above. Water content, TN, TOC, TIC, TS and Ca reveal only minor variations with low values. C/N ratios oscillate around 6. $\delta^{13}C_{org}$ values vary slightly around 26.0‰ but show two minima at 434cm and at 415cm followed by a shift to more positive values at 407cm (Fig. 5). Ti, Fe, K and Co show a prominent shift to higher values around 770cm. Decreasing values from 770 to 645cm are followed by an increase (646–397cm). Mn only shows minor fluctuations around 200cps in the whole record except for two distinct maxima at 854cm and 538cm (Fig. 5).

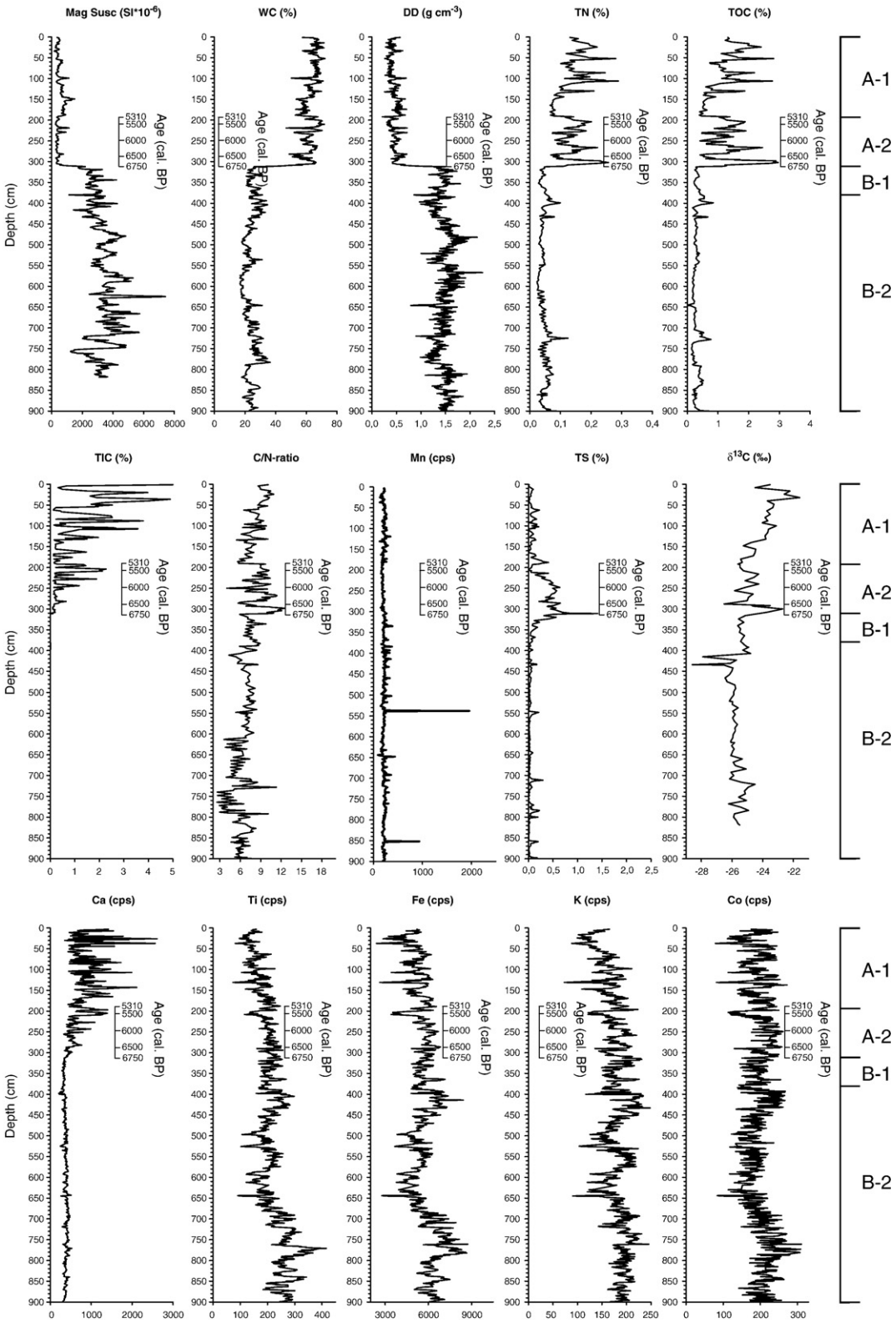

Fig. 5. Profiles of geochemical, geophysical, isotopic and XRF scanning analyses. XRF data is plotted as counts per second (cps). The age axis results from the age model (Fig. 4). Mag Susc refers to magnetic susceptibility, WC to water content and DD to dry density.

4.4.2. Unconformity visible in lithology

The most prominent shift in most parameters occurs at a sediment depth of 311 to 312cm (Fig. 5). This shift is clearly visible in magnetic susceptibility, water content, dry density, TN, TOC, TIC and Ca (Fig. 5). Below 311cm values of magnetic susceptibility and dry density are much higher than above. The opposite is observable for water content, TN, TOC, TIC, $\delta^{13}C_{org}$ and Ca with higher and oscillating values above 312cm (Fig. 5). Other data obtained by XRF scanning do not show any anomalous features at the level of the unconformity visible in the other parameters but TS, $\delta^{13}C_{org}$ and C/N exhibit a major peak.

4.4.3. Lithological unit A (above unconformity visible in lithology)

At 308cm sediment depth XRD analysis shows the presence of calcite, chamosite, illite–montmorillonite, plagioclase, pyrite and quartz. Higher in the section, TS and C/N ratios continue to show high values (TS until 164cm, C/N ratio until 190cm). At 290 and 250cm minima are observed in the C/N ratio. Towards the top of the record values are significantly lower, but C/N ratios rise again in the uppermost 50cm. TIC and related Ca show much higher variations than in unit B, increasing to the top of the core (Fig. 5). A similar pattern is observed for water content, TN and TOC, though the latter two parameters show low values between 190 and 120cm. Magnetic susceptibility and dry density show slightly higher values at the same depth, although in general, values between 311 and 0cm are low. Ti, Fe, K and Co gradually decrease from 311cm sediment depth to the top. $\delta^{13}C_{org}$ decreases to lowest values at 293cm, followed by a slight increasing trend from 290cm to 132cm. From there values rise to highest of the record between 32 and 16cm sediment depth (Fig. 5).

5. Interpretation and discussion

5.1. Chronology

An age-depth model has been established on the basis of radiocarbon dates and tephrochronological studies. The age model above the unconformity visible in the parameters and the lithology (lithological unit A-2) is based on three AMS ^{14}C dates using the medians of the 2σ-probability distribution calculated with the southern-hemisphere calibration curve (McCormac et al., 2004). A linear regression ($y = 0.0834x$ 251.8) of the three medians was calculated to form the age model ($R^2 = 0.97$, Fig. 4). The calculated ages derived from that age model for the respective depths are given in Table 1 as cal. yr BP. Based on this approach the sedimentation rate between 191 and 311cm is 0.83mm/yr.

If sedimentation had continued with the same rate (0.83mm/yr) to the top of the core, about 3000years or 3.6m would be missing. However, according to observations in the field, the sediment/water interface was well-preserved and forms the top of the sediment record (i.e., the coring date in March 2003). Therefore, either the sedimentation rate decreased after 5310cal. yr BP (191cm) to less than 0.35mm/yr (Fig. 4) or there is one large or several smaller hiatuses due to erosion or non-deposition.

A date obtained at 372cm is in the same age range as the date at 311cm (Figs. 3 and 4, Table 1). However, physical-property parameters suggest that lithological units B-1 and B-2 are similar and hence, lithological unit B-1 belongs to the lower part of the core (Fig. 5), which apparently is much older.

The dated stems of aquatic mosses yielded only 0.23mg of carbon for AMS-dating, instead of the normally necessary 1mg of carbon. Nevertheless, the age of the sample might be correct as in most cases a lower carbon content only affects precision. Accordingly, the date at 372cm was accepted and perturbation of the sediment during deposition is assumed for the section between 312 and 372cm (Fig. 4), resulting in a reworked layer. In the reworked layer, younger plant remains were incorporated into older minerogenic sediment with similar properties as the sediment deposited during OIS 3. The reworked layer was probably deposited very rapidly during a lake transgression as the shoreline passed the coring location. It was likely formed before the onset of Holocene pelagic sediment deposition.

According to the interpretation of lithological unit B-1 as a reworked layer one has to distinguish between the unconformity visible in the seismic profile and the unconformity visible in parameters and lithology which do not seem to be identical. The latter is located above unit B-1 whereas the first is probably located below.

Another possible interpretation of unit B-1 is that it is a palaeosoil. However, this is unlikely because the dates at 311cm and 372cm show only slightly different results though they are 61cm apart, and the date at 372cm was obtained from stems of aquatic mosses and not from roots. Therefore, the cover of 61cm also containing organic macro-remains (detritus), which was not in situ, must have formed very rapidly.

As the 2σ-probabilities of the dates at 311 and 372cm are overlapping and a clear boundary is visible in the proxy data (Fig. 5) and in the lithology (Fig. 3), the law of superposition, which states that the younger strata rest on older strata (Schwarzacher, 2000) is applied. Therefore,

for 372cm (Table 1) the median of the maximum age of that dating and the calculated age (i.e., cal. yr BP in Table 1) of the dating at 311cm was chosen (6790±40cal. yr BP). The reworked layer is delimited at the top by the marked shifts in all data above 312cm and at the base by an undisturbed tephra layer at 379cm.

Below 379cm sediment depth, material suitable for radiocarbon dating was found only at 728cm depth. A sample from that depth yielded an uncalibrated age of 44,800yr BP. However, no similar tephra is contained in a core from the center of Laguna Potrok Aike, continuously spanning the last 13.5kyr BP (Haberzettl, 2006, Haberzettl et al., 2007). Therefore, lithological unit B-2 at the transition between unit B-1 and B-2 seems to be older than 13.5kyr.

Based on this chronology the record can be divided into four parts (Fig. 4), which are consistent with the lithological units (Fig. 3):

1. B-2: Pleistocene (OIS 3) section dated at 45kyr BP at 728cm (900–379cm),
2. B-1: reworked layer (378–312cm),
3. A-2: mid-Holocene section of continuous sedimentation (311–191cm) dated at 6750–5310cal. yr BP,
4. A-1: late Holocene section of either low sedimentation rate (0.35mm/yr) or discontinuous sedimentation (190–0cm) without age control.

5.2. Tephrochronology

The results of tephrochronological studies suggest an origin of all three tephras from AVZ volcanoes, even though none of them can be correlated with any specific tephra event so far. The unique bimodal glass composition and mineral assemblage of the youngest tephra at 379cm sediment depth indicate an origin from Reclús volcano, even though one group of glass shards clusters in the lower field of the NAVZ products (Fig. 6). Apart from slightly higher potassium values, the major-element chemistry is similar to late Pleistocene and Holocene tephra products from Reclús volcano (Bitschene and Fernandez, 1995; Kilian et al., 2003b; Naranjo and Stern, 1998; Stern, 1990; Stern and Kilian, 1996) but differs from a 12.6kyr BP ash (McCulloch et al., 2005) intercalated in a sediment record recovered from the center of Laguna Potrok Aike (Haberzettl, 2006; Haberzettl et al., 2007). This suggests an age for tephra deposition before 13.5kyr BP (oldest part of the record from the center of the lake). The major-element chemistry of the tephras deposited at 643 and 859cm sediment depth clearly clusters within the Mt. Burney pyroclastic field, indicating an origin from this volcano (Table 2, Fig. 6). According to the preliminary age estimation described above, the tephras were erupted shortly before and after 44.8±2kyr BP. This radiocarbon

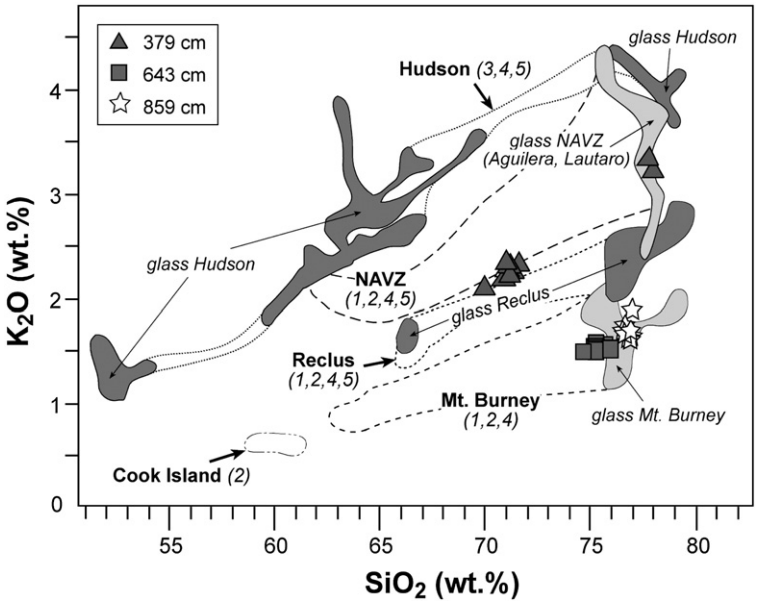

Fig. 6. Biplot of SiO_2 versus K_2O for single glass shards extracted from Laguna Potrok Aike tephras at 379 cm (triangles), 643 cm (rectangles) and 859 cm (stars) compared to the mean oxide concentrations of tephras derived from southern Patagonian volcanoes (geochemical envelopes = EPMA data of juvenile glass; dashed lines = whole rock XRF data). Data are from: (1) (Stern, 1990); (2) (Stern and Kilian, 1996); (3) (Naranjo and Stern, 1998); (4) (Kilian et al., 2003b); (5) (Bitschene and Fernandez, 1995).

date is supported by the stratigraphic position of Mt. Burney tephras in respect to the > 12.6kyr BP Reclús tephra. Even though independent dating of tephra layers is not available at the moment, the correlations of Laguna Potrok Aike tephras to distinct volcanic sources help to increase the knowledge of the explosive activity of southern Patagonian volcanoes during OIS 3. The results of tephrochronological investigations, for instance, imply that at least Reclús volcano and Mt. Burney were explosively active around 45kyr BP. According to the thicknesses of tephra layers in the Laguna Potrok Aike sediment core and the maximum grain sizes of their components, large volumes of tephra have been erupted and dispersed in an easterly direction, suggesting an occurrence of westerly winds similar to today during the last glacial period. The major-element chemistry of juvenile clast and phenocryst assemblages of tephras moreover indicates that the magma composition during the last 45ka did not significantly change at Mt. Burney, while magma erupted from Reclús volcano evolved slightly during this time period.

The tephrochronological results, however, are in agreement with the age model constrained by radiocarbon datings. The unconformity at ca. 7cal. kyr BP is confirmed by the absence of distal tephras deposited between 7cal. kyr BP and 16cal. kyr BP in the center of the lake (Haberzettl, 2006; Haberzettl et al., 2007).

5.3. Hydrological variability

The interpretation and discussion starts with an introduction to indicators for lake level changes. Subsequently, lithological unit A-2, 311–191cm, for which a good age control is available, is discussed in order to explain the interdependence of some proxies on the basis of continuous deposition. This is essential for sections without continuous age control, which will be discussed subsequently. Hence, lithological units A-2 and A-1 (Holocene) will be discussed prior to the lithological units B-2 (OIS 3) and B-1 (reworked layer).

5.3.1. Indicators for lake level changes: C/N

C/N ratios were used as an indicator of palaeoshoreline proximity for a short core from the center of Laguna Potrok Aike (Haberzettl et al., 2005) as well as for Lake Victoria, East Africa (Meyers and Teranes, 2001). C/N ratios distinguish between higher plant (aquatic macrophytes, terrestrial vegetation) and algal and soil material (Mayr et al., 2005). For Laguna Potrok Aike, this assumption is based on the knowledge that terrestrial and littoral aquatic macrophytes show high C/N ratios above 24 (Haberzettl et al., 2005) and can therefore be distinguished from planktonic algae which typically have C/N ratios between 4 and 10 (Meyers, 1997; 2003; Meyers and Teranes, 2001). Similar observations were made for Laguna Azul (Fig. 1), located approximately 60km further to the east (Mayr et al., 2005).

5.3.2. Indicators for lake level changes: stable isotopes

$\delta^{13}C_{org}$ was also identified as a sensitive parameter for palaeoshoreline proximity for Laguna Potrok Aike (Haberzettl et al., 2005) and Laguna Azul (Mayr et al., 2005). It indicates higher contributions of organic matter from aquatic macrophytes, which have $\delta^{13}C_{org}$ values between 10 and 16‰ at Laguna Potrok Aike.

5.3.3. Indicators for lake level changes: calcium carbonates

TIC and Ca represent autochthonously precipitated $CaCO_3$, which was identified as a sensitive lake-level (water volume) indicator in Laguna Potrok Aike (Haberzettl et al., 2005). Due to concentration and dilution processes, there is a relationship between those proxies and lake level: high TIC and Ca values point to a low lake level and vice versa (Haberzettl et al., 2005). This is based on calcite precipitation during concentration (= lake level lowering/low lake level) and no precipitation during times of dilution (= lake level rise/high lake level).

5.3.4. Indicators for lake level changes: titanium (Ti), iron (Fe), potassium (K) and cobalt (Co)

In many aquatic systems allochthonous clastic input is characterized by higher Ti and Fe contents (Haug et al., 2003). For Laguna Potrok Aike correlations of Ti with Fe, K and Co (R^2 = 0.69, 0.65 and 0.50) allow the same conclusion for K and Co. At this lake, the allochthonous input is associated with run-off and hence hydrological variability (Haberzettl et al., 2005).

5.3.5. Lithological unit A-2

Lithological unit A-2 represents the first continuously deposited Holocene sediment at the core site. This means that the lake level above the terrace after the transgression was high enough to prevent disturbances at the sediment surface. The core site was well below wave base, which is estimated to be in a water depth of 3–5m (Sly, 1994) if preconditions given at Laguna Potrok Aike are taken into account. Today, aquatic macrophytes start to grow at a water depth of 2 to 3m, suggesting recent disturbances to that depth. Hence, the lake level at least had to be 3m above the core site. However, as indicated by higher TIC, TOC, TN and C/N ratios, the lake level was still quite low in

comparison to lithological unit B and the lower part of A-1.

In Laguna Potrok Aike, C/N ratios between 311 and 290cm (6750–6500cal. yr BP) are highest (Fig. 5) and reflect higher contributions of terrestrial and aquatic macrophytes, i.e., a rising lake level still close to the coring location. High peaks in TN and TOC during that time (Fig. 5) point towards erosion of plants at the littoral belt by wave action and accumulation at the coring location. Further evidence for this is given by the higher amount of plant debris in this core section (Fig. 3). The interpretation of a shoreline close to the coring location in the lake (similar elevation) is supported by the $\delta^{13}C_{org}$ values (Fig. 5). The most positive $\delta^{13}C_{org}$ values of unit A-2 are observed between 311cm and 290cm (6750–6500cal. yr BP), possibly indicating higher contributions of organic matter from aquatic macrophytes. Thus, shallow-water habitats in which the aquatic macrophytes live still were close to the coring location (Fig. 5). TIC and Ca support a rising lake level (Fig. 5) in this interval. In this case low values probably indicate a lake-level rise with minor stagnations or lake level lowerings, which cause brief intervals of low $CaCO_3$ precipitation. Therefore, according to all parameters, between 6750 and 6500cal. yr BP lake level was rising to an elevation only slightly but at least 3m above the core site.

Around 290cm (6500cal. yr BP) all parameters indicate a distinctly higher lake level than before (Fig. 5). This is also true for indicators of minerogenic input (Ti, Fe, K, Co) which show the highest values of the entire Holocene around 290cm (ca. 6500cal. yr BP) indicating enhanced fluvial detrital input and hence, a higher lake level.

Above 290cm, until 191cm (6500–5310cal. yr BP) all proxies oscillate rapidly indicating a variable lake level (Fig. 5). However, minerogenic input indicators show a trend to lower input. Ca and TIC support a lake level lowering or stagnation at ca. 5500cal. yr BP.

Elevated TS values indicate oxygen-poor to anoxic conditions in the sediment of unit A-2 (Fig. 5). This assumption is based on an XRD analysis at 308cm sediment depth, which reveals the presence of pyrite (FeS_2). Therefore, it is assumed that the sulfur present in this section is mainly incorporated into pyrite, which forms under oxygen-restricted conditions (Wignall et al., 2005) in association with the decomposition of organic matter (Gore, 1988). This does not necessarily imply that the lake water above the sediment was anoxic (Gore, 1988), as pyrite can also form below the sediment/water interface in organic-rich sediments deposited in oxygenated water (Cohen, 2003; Gore, 1988). By rapid deposition of minerogenic matter (indicated e.g., by Ti) an oxygen-impermeable layer may develop. The impermeable layer leads to anaerobic decomposition of deposited organic matter in interstitial waters, resulting in reducing anaerobic conditions (O'Neil, 1998). This can induce pyrite formation (Degens, 1968; Wignall et al., 2005). Therefore, the preservation of TS as FeS_2 is dependent on the minerogenic input. As Ti, Fe, K and Co and hence minerogenic input decrease, e.g., around 200cm (ca. 5500cal. yr BP), TS decreases as well.

5.3.6. Lithological unit A-1

There are two possible reasons for the distinct change in sedimentation rate above 191cm (Fig. 4): (1) sediment supply was significantly reduced, either due to a higher lake level increasing the distance to the shore and thus leading to decreased sedimentation or due to less direct input to the lake; (2) regressions of lake level created the formation of unconformities. Considering a constant sedimentation rate and interruptions in sedimentation (non-deposition) without significant phases of erosion, the sum of the breaks would have lasted approximately 3000 years. This value is derived from the intersection of the extrapolated regression of the dated Holocene section (unit A-2) with the sediment surface (Fig. 4). Accordingly, if erosion is considered as well, this time span would be shorter.

Neither lithology (Fig. 3) nor seismic reflection investigations (e.g., Fig. 2) indicate any evidence for unconformities in this lithological unit. Attempts to correlate this section with cores from the center of the lake (Mayr et al., unpublished data) with respect to $\delta^{13}C_{org}$ reveal a similar trend. Hence, a constant but lower sedimentation rate than in lithological unit A-2 can be assumed for unit A-1 which is also indicated by low TS values.

The low values of TIC, C/N ratio, TOC, TN and $\delta^{13}C_{org}$ (Fig. 5) at the bottom of this unit and the trend to higher values towards the top, beginning at 132cm sediment depth, point to an initially high lake level followed by a regression. A lower lake level close to the top of the core becomes especially evident if $\delta^{13}C_{org}$ is considered (Fig. 5): at 311cm, the depth where undisturbed Holocene sedimentation began, values for this palaeoshoreline proximity indicator are very high. At that time the lake shore was likely close to the coring location causing high $\delta^{13}C_{org}$ values due to deposition of aquatic macrophytes. At a depth of 16 to 32cm, values for $\delta^{13}C_{org}$ are even higher (Fig. 5) implying that the lake shore was also very close to the core site and aquatic macrophyte debris was deposited. Toward the

top of the core, Ti, Fe, K and Co also suggest less minerogenic sediment supply and hence less fluvial input and drier conditions (Fig. 5).

Due to the lack of datable material it was impossible to determine the regression in greater temporal detail. The most likely scenario for this interval includes increasing the distance to the shore, and hence leading to lower rates of deposition followed by a regression with less minerogenic input resulting in a constant but lower sedimentation. The record from the center of Laguna Potrok Aike (Fig. 2) also shows a transgression followed by a trend towards a lower lake level during the late Holocene (Haberzettl, 2006; Haberzettl et al., 2007). This is in agreement with the absence of glacier extensions greater in extent than the "Little Ice Age" moraines during the last 5000 years at Gran Campo Nevado (53° S, Fig. 1) located southwest of Laguna Potrok Aike, which might also be attributed to drier conditions (Kilian et al., 2003a).

5.3.7. Lithological unit B-2

Assuming that during glacial times $\delta^{13}C_{org}$, TIC, Ca and C/N ratio can be used as lake-level indicators in the same way as in the Holocene, the lake level during OIS 3 (Fig. 5) was the highest of the record. The high lake level during that time may point to a less arid climate or less evaporation (due to e.g., higher relative humidity, less wind resulting in less evaporation or seasonal ice cover). A high lake level of Laguna Potrok Aike at this time coincides with lower dust values than during OIS 4 and 2 in the Vostok and Epica ice core records, where the source of the dust was ascribed to Patagonia (Delmonte et al., 2004; Basile et al., 1997; Petit et al., 1999; 1999). This implies that the source area was wetter during OIS 3 than during OIS 4 and 2 hampering dust mobilization despite the lack of vegetation. If the lake level could be attributed to increased precipitation, an increase of precipitation-bearing easterly winds can also be assumed (Haberzettl, 2006; Mayr et al., 2007; Schneider et al., 2003). This implies a reduction of the intensity of the strong westerly winds, which are probably responsible for dust transport at a larger scale (e.g., Antarctica). However, a prevalence of westerly winds can be concluded from the presence of the tephra layers explaining the higher dust contents than today due to less vegetated and easily erodible ground in Patagonia. An unlikely scenario might be the development of a vegetation cover impeding dust mobilization more effectively. However, due to the cold conditions assumed for the glacial period this is unlikely. The generally higher values of Ti, Fe, K and Co in Laguna Potrok Aike are further evidence for this hypothesis, and might be explained by the fact that during colder conditions vegetation cover was markedly reduced. Therefore, material in the catchment was eroded and transported to the lake.

The reduced plant cover might also be responsible for high values of dry density and magnetic susceptibility (Fig. 5), both commonly associated with allochthonous input (Geiss et al., 2003; Thompson et al., 1975). At Laguna Potrok Aike OIS 3 sediments consist of coarse silt and fine sand (Fig. 7). This sediment fraction is the first fraction to be moved by wind and kept in suspension (Tucker, 1991). Magnetic susceptibility varies with the magnetite grain size, usually showing distinct maxima at around 0.02μm and between 25 and 100μm (Dearing, 1994). The latter spectrum matches with the peak of the grain-size distribution of the OIS 3 section in Laguna Potrok Aike (Fig. 7). Between the two areas of increased magnetic susceptibility values are rather low. This is in agreement with the mean grain-size distribution above the unconformity visible in proxies and lithology in Laguna Potrok Aike, which is almost equally distributed from 0.4 to 200μm (Fig. 7). Though the interval between 25 and 100μm is also contained in the grain-size distribution above the unconformity, there is a dilution effect by material of smaller grain sizes (Fig. 7). Due to the reduced vegetation cover higher amounts of dust should have been transported to the lake compared to Holocene times. This would be in agreement with higher amounts of dust during OIS 3 than today in the Vostok record (Petit et al., 1999; 1990) though it is less than during OIS 4 or 2. Comparisons between the Vostok ice core record and magnetic susceptibility measured on a loess sequence in China showed similar results, with high magnetic-susceptibility values during glacial periods with loess accumulation (= dust maxima in ice core) and low magnetic-susceptibility values in interglacial soils (Petit et al., 1990). If the origin of the sediments deposited during OIS 3 could be mainly attributed to aeolian transport of loess-like material, this would explain the higher values of magnetic susceptibility as this parameter may register changing sediment sources for lake sediments or a different transport mechanism (Dearing, 1994). In this case, magnetic susceptibility might be used as a dust indicator. Unfortunately, neither sediment from the Last Glacial Maximum (OIS 2) nor from OIS 4, when dust fluxes were even higher in the Vostok record (Petit et al., 1999; 1990), have been recovered from Laguna Potrok Aike to test whether magnetic-susceptibility values were higher during those times.

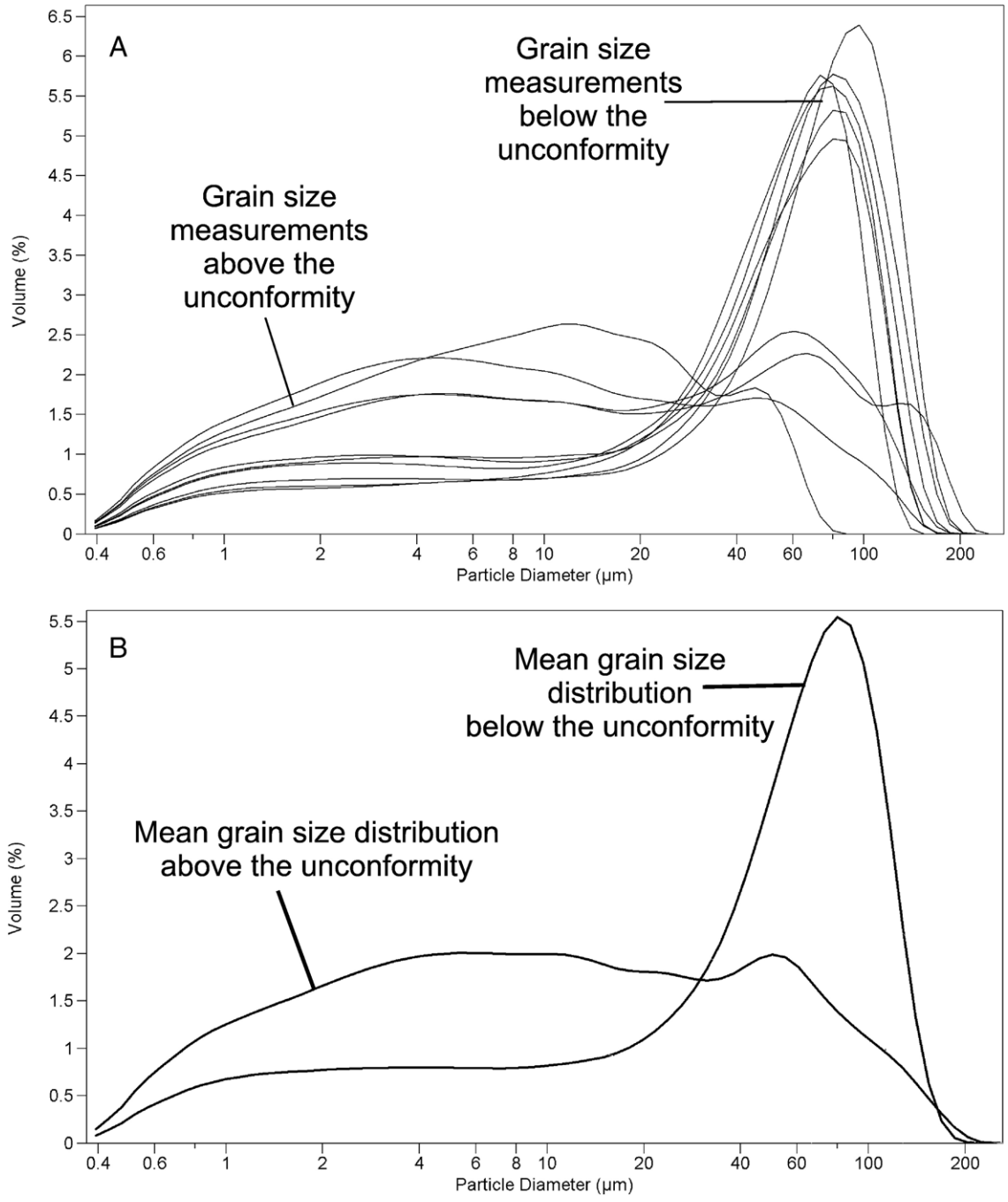

Fig. 7. Differences in grain size distribution above and below the unconformity visible in parameters (Fig. 5) and lithology (Fig. 3). In A all measurements are displayed, B shows the mean grain-size distribution. Note different scaling in A and B.

5.3.8. Lithological unit B-1

There is conflicting evidence for the exact thickness of the reworked layer. As far as $\delta^{13}C_{org}$, C/N ratio, TOC, TN, Ca, Ti, Fe, K and Co are concerned, it seems to proceed from 312 to 407cm. At this depth, a distinct change takes place in those parameters. Between 312 and 407cm values are almost constant (Fig. 5). However, at 379cm a tephra layer was found. If the sediment was already in a state of mixing, this tephra would have been reworked and probably been diluted. Furthermore, below the tephra no organic macrophytes were detected whereas there were plenty above it (Fig. 3). Therefore,

the tephra is interpreted as definite lower boundary of the reworked layer. However, the true boundary may be slightly above the tephra. The change in the proxies at 407cm sediment depth hence has to be attributed to a different event. After this event, sedimentation continued until the tephra was deposited. Due to erosion, mixing and (re)deposition, the homogeneity, visible in almost all proxies of lithological unit B-1, can be explained (Fig. 5).

The radiocarbon date of 6790±40cal. yr BP in lithological unit B-1 indicates when climate became more humid. This resulted in a significant lake-level rise leading to erosion of a mixture of mid-Holocene plant macro-remains and eroded OIS 3 minerogenic sediments, and deposition onto much older OIS 3 material as the lake shore passed by during transgression. The age of 6790±40cal. yr BP is a minimum age of the onset of transgression, because the lake level might have been lower than the 30m level of the coring site. During the previous dry phase, the lake level either dropped to or below the lake-level terrace and eroded parts of the previously deposited sediment section. This formed the reworked layer and the erosional unconformity visible in proxies and lithology marking the transition from the reworked layer to Holocene sedimentation between 311 and 312cm sediment depth in the proxies.

The occurrence of the dry phase prior to 6790±40cal. yr BP is in agreement with analyses of sediment cores (Gilli, 2003; Markgraf et al., 2003) from Lago Cardiel (49° S) which yield evidence for an increased influx of freshwater into the lake between 7100 and 5500cal. yr BP (Gilli, 2003). The core from the center of Laguna Potrok Aike also points to a lake-level lowstand after 8650nhcal. yr BP (Haberzettl, 2006; Haberzettl et al., 2007).

6. Conclusions

The sediment record from the sub-aquatic lake-level terrace of Laguna Potrok Aike can be divided into four lithological units: a Pleistocene section (OIS 3, B-2) with an age of about 45kyr BP, a reworked layer (B-1), a well-dated mid-Holocene section (A-2) covering the time interval from 6750 to 5310cal. yr BP, and a section without a confirmed age control due to a lack of aquatic macrophytes suitable for dating above (late Holocene, A-1). High lake levels are interpreted during OIS 3 from results of a multi-proxy study of sediment core PTA03/6 indicating sediment deposition at more than 70m above the modern lake floor. This sediment core extends the sediment record from the center of Laguna Potrok Aike covering the last 13.5kyr BP (16,000cal. yr BP) further back in time and emphasizes the potential of Laguna Potrok Aike for long-term palaeoclimate reconstructions. In comparison to the Holocene section, however, geochemical indicators of dominant allochthonous material point towards a different sediment source or to a different transport mechanism that likely developed when the catchment had sparse vegetation cover during OIS 3. Sediment deposited between OIS 3 and 6790cal. yr BP was probably eroded during lake-level lowstands.

The radiocarbon date of 6790cal. yr BP in the reworked layer gives a minimum age for a hydrological change, leading to a higher lake level, as the rising lake level needed some time to reach the elevation of the coring location. This event caused an unconformity visible in seismic profiles, showing sediments dipping towards the lake center below the unconformity, and horizontally-laminated sediments above. Due to the reworked layer, the seismic unconformity is not visible in the sedimentological parameters. Therefore, the unconformity visible in proxies and lithology is at the top of the reworked layer (311–312cm).

The lake level was stable and stayed near the elevation of the coring location (i.e., 70m above present lake floor) or was slowly rising until 6500cal. yr BP, then rose considerably. Subsequently, lake level was variable, but receding. Around 5310cal. yr BP lake level rose again and some time after 5310cal. yr BP climate became drier. After that date no material suitable for radiocarbon dating was found, which inhibits a precise dating of the regression. Climate proxies indicate less minerogenic sediment supply to the lake after 5310cal. yr BP which may explain the low sedimentation rate.

Three tephra layers, none previously described, were recovered from PTA03/6 and are restricted to the Pleistocene. Geochemical and petrophysical data indicate that these tephras are derived from the Mt. Burney and Reclús volcanoes. These results imply that at least the AVZ volcanoes were explosively active around 45kyr BP, and thus, there is a high potential for tephrostratigraphical studies in southern Patagonia and the western part of the South-Atlantic Ocean that requires further volcanological and tephrochronological efforts.

Acknowledgements

We would like to recognize the significant help Gustavo Villarosa and guest editor Marc De Batist provided in their comments which improved this manuscript. We are much indebted to Holger Wissel for technical assistance with stable-isotope analyses and Sabine Stahl, Benjamin Bünning, Sabine Wrocklage and Tim Haarmann for assistance with geochemical analyses. For the storage of sediment cores at the IODP/ODP Bremen Core

Repository and for providing technical equipment and know-how we would like to thank Walter Hale, Heike Pfletschinger, Ursula Röhl and Alexius Wülbers. We are much obliged to Thomas Frederichs and Christian Hilgenfeldt for putting us the Bartington sensor at our disposal. Adrian Gilli is acknowledged for the provision with tephra samples from the Lago Cardiel sediment record. We would also like to thank ZEKAM, University of Bremen, for performing XRD analyses. Christobal Kennard, Capt. Jorge D. Moreteau and the staff of INTA, Río Gallegos, are acknowledged for organizing the logistics of the field work. This is a contribution to the German Climate Research Program DEKLIM (01 LD 0034 and 0035) of the German Federal Ministry of Education and Research (BMBF).

References

Auer, V., 1974. The isorythmicity subsequent to the Fuego-Patagonian and Fennoscandian ocean level transgression of the latest glaciation. Annales Academiae Scientiarum Fennicae Series A, 3 115, 1–188.

Basile, I., Grousset, F.E., Revel, M., Petit, J.R., Biscaye, P.E., Barkov, N.I., 1997. Patagonian origin of glacial dust deposited in East Antarctica (Vostok and Dome C) during glacial stages 2, 4 and 6. Earth and Planetary Science Letters 146, 573–589.

Bitschene, P.R., Fernandez, M.I., 1995. Volcanology and petrology of fallout ashes from the August 1991 eruption of the Hudson volcano (Patagonian Andes) In: Bitschene, P.R., Mendia, J. (Eds.), The August 1991 Eruption of the Hudson Volcano (Patagonian Andes): a Thousand Days After. Cuvillier, Göttingen, pp. 27–54.

Cohen, A.S., 2003. Paleolimnology. The History and Evolution of Lake Systems. Oxford University Press, Oxford.

Dearing, J., 1994. Environmental Magnetic Susceptibility. Using the Bartington MS2 System. Chi Publishing, Kentworth.

Degens, E.T., 1968. Geochemie der Sedimente. Ferdinand Enke Verlag, Stuttgart.

Delmonte, B., Basile-Doelsch, I., Petit, J.R., Maggi, V., Revel-Rolland, M., Michard, A., Jagoutz, E., Grousset, F., 2004. Comparing the Epica and Vostok dust records during the last 220,000years: stratigraphical correlation and provenance in glacial periods. Earth-Science Reviews 66, 63–87.

Endlicher, W., 1993. Klimatische Aspekte der Weidedegradation in Ost-Patagonien In: Hornetz, B., Zimmer, D. (Eds.), Beiträge zur Kultur- und Regionalgeographie. Festschrift für Ralph Jätzold. Trierer Geographische Studien. Geographische Gesellschaft Trier, Trier, pp. 91–103.

Geiss, C.E., Umbanhowar, C.E., Camill, P., Banerjee, S.K., 2003. Sediment magnetic properties reveal Holocene climate change along the Minnesota prairie-forest ecotone. Journal of Paleolimnology 30, 151–166.

Gilli, A., 2003. Tracking late Quaternary environmental change in southernmost South America using lake sediments of Lago Cardiel (49°S), Patagonia, Argentina. Ph.D. thesis. No. 15307, ETH Zürich, Switzerland.

Gilli, A., Anselmetti, F., Ariztegui, D., Bradbury, J., Kelts, K., Markgraf, V., McKenzie, J., 2001. Tracking abrupt climate change in the Southern Hemisphere: a seismic stratigraphic study of Lago Cardiel, Argentina (49°S). Terra Nova 13, 443–448.

Gilli, A., Anselmetti, F.S., Ariztegui, D., Beres, M., McKenzie, J.A., Markgraf, V., 2005. Seismic stratigraphy, buried beach ridges and contourite drifts: the Late Quaternary history of the closed Lago Cardiel basin, Argentina (49°S). Sedimentology 52, 1–23.

Gore, P.J.W., 1988. Lacustrine sequences in an early Mesozoic rift basin: Culpeper Basin, Virginia, USA In: Fleet, A.J., Kelts, K., Talbot, M.R. (Eds.), Lacustrine Petroleum Source Rocks. Geological Society Special Publication. Blackwell Scientific Publications, Oxford, pp. 247–278.

Haberle, S.G., Lumley, S.H., 1998. Age and origin of tephras recorded in postglacial lake sediments in the west of the southern Andes, 44°S to 47°S. Journal of Volcanology and Geothermal Research 84, 239–256.

Haberzettl, T., 2006. Late Quaternary hydrological variability in southeastern Patagonia — 45,000years of terrestrial evidence from Laguna Potrok Aike. Ph.D. thesis. University of Bremen, Germany. http://nbn-resolving.de/urn:nbn:de:gbv:46-dis000103918.

Haberzettl, T., Fey, M., Lücke, A., Maidana, N., Mayr, C., Ohlendorf, C., Schäbitz, F., Schleser, G.H., Wille, M., Zolitschka, B., 2005. Climatically induced lake level changes during the last two millennia as reflected in sediments of Laguna Potrok Aike, southern Patagonia (Santa Cruz, Argentina). Journal of Paleolimnology 33, 283–302.

Haberzettl, T., Wille, M., Fey, M., Janssen, S., Lücke, A., Mayr, C., Ohlendorf, C., Schäbitz, F., Schleser, G.H., Zolitschka, B., 2006. Environmental change and fire history of southern Patagonia (Argentina) during the last five centuries. Quaternary International 158, 72–82.

Haberzettl, T., Corbella, C., Fey, M., Janssen, S., Lücke, A., Mayr, C., Ohlendorf, C., Schäbitz, F., Schleser, G.H., Wille, M., Wulf, S., Zolitschka, B., (2007). Lateglacial and Holocene wet-dry cycles in southern Patagonia: chronology, sedimentology and geochemistry of a lacustrine sediment record from Laguna Potrok Aike, Argentina. The Holocene 17, 297–310.

Haug, G., Gunther, D., Peterson, L., Sigman, D., Hughen, K., Aeschlimann, B., 2003. Climate and the collapse of Maya civilization. Science 299, 1731–1735.

Heusser, C.J., Heusser, L.E., 2006. Submillennial palynology and palaeoecology of the last glaciation at Taiquemo (~50,000 cal yr, MIS 2–4) in southern Chile. Quaternary Science Reviews 25, 446–454.

Heusser, L., Heusser, C.J., Kleczkowski, A., Crowhurst, S., 1999. A 50,000-yr pollen record from Chile of South American millennial-scale climate instability during the last glaciation. Quaternary Research 52, 154–158.

Heusser, C.J., Lowell, T.V., Heusser, L.E., Moreira, A., Moreira, S., 2000. Pollen sequence from the Chilean Lake District during the Llanquihue glaciation in marine Oxygen Isotope Stages 4-2. Journal of Quaternary Science 15, 115–125.

Hunt, J.B., Hill, P.G., 1996. An inter-laboratory comparison of the electron probe microanalysis of glass geochemistry. Quaternary International 34-36, 229–241.

Jansen, J.H.F., van der Gaast, S.J., Kloster, B., Vaars, A.J., 1998. CORTEX, a shipboard XRF-scanner for element analyses in split sediment cores. Marine Geology 151, 143–153.

Kilian, R., Fresq-Martin, M., Schneider, C., Biester, H., Casassa, G., Arévalo, M., Wendt, G., Behrmann, J., 2003a. Late glacial ice retreat in the southernmost Andes: sedimentological and palynological implications. 10 Congreso Geológico Chileno, Concepción, p. 5.

Kilian, R., Hohner, M., Biester, H., Wallrabe-Adams, H.J., Stern, C., 2003b. Holocene peat and lake sediment tephra record from the

southernmost Chilean Andes (53–55°S). Revista Geologica de Chile 30, 23–37.

Le Bas, M.J., Le Maitre, R.W., Streckeisen, A., Zanettin, B., 1986. A chemical classification of volcanic rocks based on the Total Alkali–Silica diagram. Journal of Petrology 27, 745–750.

Markgraf, V., Bradbury, J.P., Schwalb, A., Burns, S.J., Stern, C., Ariztegui, D., Gilli, A., Anselmetti, F.S., Stine, S., Maidana, N., 2003. Holocene palaeoclimates of southern Patagonia: limnological and environmental history of Lago Cardiel, Argentina. Holocene 13, 581–591.

Mayr, C., Fey, M., Haberzettl, T., Janssen, S., Lücke, A., Maidana, N., Ohlendorf, C., Schäbitz, F., Schleser, G.H., Struck, U., Wille, M., Zolitschka, B., 2005. Palaeoenvironmental changes in southern Patagonia during the last millennium recorded in lake sediments from Laguna Azul (Argentina). Palaeogeography, Palaeoclimatology, Palaeoecology 228, 203–227.

Mayr, C., Wille, M., Haberzettl, T., Fey, M., Janssen, S., Lücke, A., Ohlendorf, C., Oliva, G., Schäbitz, F., Schleser, G.H., Zolitschka, B., 2007. Holocene variability of the Southern Hemisphere westerlies in Argentinean Patagonia (52°S). Quaternary Science Reviews 26, 579–584.

McCormac, F., Hogg, A., Blackwell, P., Buck, C., Higham, T., Reimer, P., 2004. SHCal104 Southern Hemisphere Calibration 0- 11.0 cal kyr BP. Radiocarbon 46, 1087–1092.

McCulloch, R.D., Fogwill, C.J., Sugden, D.E., Bentley, M.J., Kubik, P.W., 2005. Chronology of the last glaciation in Central Strait of Magellan and Bahía Inútil, Southernmost South America. Geografiska Annaler, Series A: Physical Geography 87, 289–312.

Meyers, P.A., 1997. Organic geochemical proxies of paleoceanographic, paleolimnologic, and paleoclimatic processes. Organic Geochemistry 27, 213–250.

Meyers, P.A., 2003. Applications of organic geochemistry to paleolimnological reconstructions: a summary of examples from the Laurentian Great Lakes. Organic Geochemistry 34, 261–289.

Meyers, P.A., Teranes, J.L., 2001. Sediment organic matter. In: Last, W.M., Smol, J.P. (Eds.), Tracking Environmental Change Using Lake Sediments. Physical and Geochemical Methods, vol. 2. Kluwer Academic Publishers, the Netherlands, pp. 239–269.

Naranjo, J.A., Stern, C.R., 1998. Holocene explosive activity of Hudson Volcano, southern Andes. Bulletin of Volcanology 59, 291–306.

O'Neil, P., 1998. Chemie der Geo-Bio-Sphäre. Natürliche Vorgänge und Auswirkungen menschlicher Eingriffe. Ferdinand Enke Verlag, Stuttgart.

Petit, J.R., Mourner, L., Jouzel, J., Korotkevich, Y.S., Kotlyakov, V.I., Lorius, C., 1990. Palaeoclimatological and chronological implications of the Vostok core dust record. Nature 343, 56–58.

Petit, J.R., Jouzel, J., Raynaud, D., Barkov, N.I., Barnola, J.M., Basile, I., Bender, M., Chappellaz, J., Davis, M., Delaygue, G., Delmotte, M., Kotlyakov, V.M., Legrand, M., Lipenkov, V.Y., Lorius, C., Pepin, L., Ritz, C., Saltzman, E., Stievenard, M., 1999. Climate and atmospheric history of the past 420,000 years from the Vostok ice core, Antarctica. Nature 399, 429–436.

Reimer, P.J., Baillie, M.G.L., Bard, E., Bayliss, A., Beck, J.W., Bertrand, C.J.H., Blackwell, P.G., Buck, C.E., Burr, G.S., Cutler, K.B., Damon, P.E., Edwards, R.L., Fairbanks, R.G., Friedrich, M., Guilderson, T.P., Hogg, A.G., Hughen, K.A., Kromer, B., McCormac, G., Manning, S., Ramsey, C.B., Reimer, R.W., Remmele, S., Southon, J.R., Stuiver, M., Talamo, S., Taylor, F.W., van der Plicht, J., Weyhenmeyer, C.E., 2004. IntCal04 terrestrial radiocarbon age calibration, 0–26 cal kyr BP. Radiocarbon 46, 1029–1058.

Roig, F.A., Le-Quesne, C., Boninsegna, J.A., Briffa, K.R., Lara, A., Grudd, H., Jones, P.D., Villagran, C., 2001. Climate variability 50,000 years ago in mid-latitude Chile as reconstructed from tree rings. Nature 410, 567–570.

Schäbitz, F., Paez, M.M., Mancini, M.V., Quintana, F., Wille, M., Corbella, H., Haberzettl, T., Lücke, A., Prieto, A., Maidana, N., Mayr, C., Ohlendorf, C., Schleser, G.H., Zolitschka, B., 2003. Estudios paleoambientales en lagos volcánicos en la Región Volcánia de Pali Aike, sur de Patagonia (Argentina): palinología. Revista del Museo Argentino de Ciencias Naturales, Nueva Serie 5, 301–316.

Schneider, C., Glaser, M., Kilian, R., Santana, A., Butorovic, N., Casassa, G., 2003. Weather observations across the southern Andes at 53°S. Physical Geography 24, 97–119.

Schwarzacher, W., 2000. Repetitions and cycles in stratigraphy. Earth-Science Reviews 50, 51–75.

Sly, P.G., 1994. Sedimentary processes in lakes. In: Pye, K. (Ed.), Sediment Transport and Depositional Processes. Blackwell, Oxford, pp. 157–191.

Stern, C.R., 1990. Tephrochronology of southernmost Patagonia. National Geographic Research 6, 110–126.

Stern, C.R., Kilian, R., 1996. Role of subducted slab, mantle wedge and continental crust in the generation of adakites from the Andean Austral Volcanic Zone. Contribution to Mineralogy and Petrology 123, 263–281.

Stern, C.R., Futa, K., Muehlenbachs, K., 1984. Isotope and trace element data for orogenic andesites from the Austral Andes. In: Harmon, R.S., Barreiro, B.A. (Eds.), Andean Magmatism: Chemical and Isotopic Constraints. Shiva, Cheshire, pp. 31–46.

Stuiver, M., Reimer, P., 1993. Extended 14C database and revised CALIB radiocarbon calibration program. Radiocarbon 35, 215–230.

Stuiver, M., Reimer, P., Reimer, R., 2005. Calib 5.0 [WWW program and documentation]. 25 May 2005.

Thompson, R., Battarbee, R.W., O'Sullivan, P.E., Oldfield, F., 1975. Magnetic susceptibility of lake sediments. Limnology and Oceanography 20, 687–698.

Toms, P.S., King, M., Zarate, M.A., Kemp, R.A., Foit, J.F.F., 2004. Geochemical characterization, correlation, and optical dating of tephra in alluvial sequences of central western Argentina. Quaternary Research 62, 60–75.

Tucker, M.E., 1991. Sedimentary Petrology: an Introduction to the Origin of Sedimentary Rocks. Blackwell Science Publications, Cambridge.

Voelker, A.H.L., 2002. Global distribution of centennial-scale records for Marine Isotope Stage (MIS) 3: a database. Quaternary Science Reviews 21, 1185–1212.

Weinelt, M., 1996-2004. Online Map Creation. 29 May 2006.

Wignall, P.B., Newton, R., Brookfield, M.E., 2005. Pyrite framboid evidence for oxygen-poor deposition during the Permian–Triassic crisis in Kashmir. Palaeogeography, Palaeoclimatology, Palaeoecology 216, 183–188.

Zolitschka, B., Schäbitz, F., Lücke, A., Wille, M., Mayr, C., Ohlendorf, C., Anselmetti, F., Ariztegui, D., Corbella, H., Ercolano, B., Fey, M., Haberzettl, T., Maidana, N., Oliva, G., Paez, M., Schleser, G.H., 2004. Climate changes in Southern Patagonia (Santa Cruz, Argentina) inferred from lake sediments: the multi-proxy approach of SALSA. Pages Newsletter 12, 9–11.

Zolitschka, B., Schäbitz, F., Lücke, A., Corbella, H., Ercolano, B., Fey, M., Haberzettl, T., Janssen, S., Maidana, N., Mayr, C., Ohlendorf, C., Oliva, G., Paez, M.M., Schleser, G.H., Soto, J., Tiberi, P., Wille, M., 2006. Crater lakes of the Pali Aike Volcanic Field as key sites for paleoclimatic and paleoecological reconstructions in southern Patagonia, Argentina. Journal of South American Earth Sciences 21, 294–309.